Supporting information for:

Evidence for an L_3 phase in ternary deep eutectics: composition-induced L_3-to-L_α transition of AOT

Dr. Oliver S. Hammond[a,§,*], Dr. Naomi S. Elstone[a,∞], Dr. James Doutch[b], Dr. Peixun Li,[b] and Prof. Karen J. Edler[a,c]

[a] Centre for Sustainable Chemical Technologies & Department of Chemistry, University of Bath, Claverton Down, Bath BA2 7AY (UK)

[b] ISIS Neutron & Muon Source, Science and Technology Facilities Council, Rutherford Appleton Laboratory, Harwell-Oxford OX11 0QX (UK)

[c] Centre for Analysis and Synthesis, Department of Chemistry, Lund University, Lund 221 00 (Sweden)

§ Current address: Department of Biological and Chemical Engineering, Aarhus University, Aarhus C 8000 (Denmark)

[∞] Current address: Department of Chemistry, University of York, Heslington YO10 5DD (UK)

*Email: oliver.s.hammond@bath.edu

Experimental Details

Sample preparation

Choline chloride (ChCl; ≥99%, Fisher), urea (≥99%, Sigma-Aldrich), d_4-urea ($CO(ND)_2$, 99.6% purity, 99.8 atom-% D, QMX laboratories), and d_9-choline chloride ($(CD_3)_3N(CH_2)_2OHCl$, ≥99% purity, QMX laboratories) were dried under vacuum at 80°C before preparation of the pure DES, which was done by mixing at 60°C until homogenized. Hydrated samples were made by addition of aliquots of the desired quantity of D_2O or milli-Q H_2O (Elga, 18.2 MΩ) to achieve the desired molar ratio. Both protonated and d_{34}-dioctyl sodium sulfosuccinate (AOT; deuterated sample prepared and provided by ISIS Deuteration Facility) were dried under vacuum at 80°C prior to measurement. Surfactant-in-DES samples were heated to 60°C and repeatedly vortexed until homogenized. Due to the precious nature of the deuterated DES and surfactant, water content could not be measured, and was not specifically controlled beyond vacuum drying. However, this methodology has been found to routinely produce samples of 'pure, dry' ChCl:urea with 2000 ppm or less, or at most 0.4 mol%, of absorbed atmospheric H_2O.[1]

Small-angle neutron scattering (SANS)

SANS measurements were carried out on the diffractometer SANS2D, at TS2 of the STFC-ISIS Neutron & Muon Source, Harwell-Oxford, UK, with access awarded under beamtime allocation RB1610337. SANS2D is a time-of-flight scattering instrument, which was operated here using neutrons of wavelength 12 Å ≥ λ ≥ 1.5 Å, with the detectors in the 4-metre configuration, giving an accessible q-range of 0.972 ≥ q ≥ 0.004 $Å^{-1}$. Samples were measured until the integrated total incident beam current exposure was 10 – 20 μA.h. A set of sample backgrounds were collected of pure DES, or DES:water mixtures where *w* (DES molar hydration ratio) varied from 0, 1, 2, 5, and 10, for ChCl:urea:water contrasts of D:D:D, H:D:D, D:H:D, and D:D:H.

A series of samples of the surfactant AOT in the ChCl:urea:water systems was prepared, at 1 wt.%, 2 wt.% and 5 wt.% of surfactant. These concentrations were measured for ChCl:urea:water:AOT-tail contrasts of D:D:D:H, H:D:D:D, and D:H:D:D, at water contents of 0, 1, 2, 5, and 10*w*. Data were treated and reduced using Mantid, and then measured sample backgrounds were subtracted, yielding datasets amenable for fitting.

Data analysis

In the first instance, the scattering length densities (SLD) for AOT, ChCl, Urea, and water, were either derived from previous reports, or calculated from the atomic scattering lengths and molecular volumes of choline chloride, urea, and AOT, through the group contribution method.[2,3] AOT tails in the micelle core were modelled either as C_8H_{17} or C_8D_{17} units, with calculated respective SLDs of -0.395×10^{-6} Å^{-2} and 6.317×10^{-6} Å^{-2}. The AOT sulfosuccinate headgroup was always protonated, and assuming that Na^+ is bound, the SLD was determined to be 3.408×10^{-6} Å^{-2}. The solvent SLDs varied for each contrast and water composition, and are shown in Table S1.

Table S1. SLDs calculated for each measured solvent composition. Since the solvent SLD is composition-dependent but the AOT tail SLD stays the same, the Δ_{SLD}; *i.e.* the scattering contrast difference between bulk solvent and micelle, generally decreased as water content increased for these systems.

[*w*] [mol. eqv.]	**Contrast [ChCl:urea :(water)]**	**SLD [x10^{-6} Å^{-2}]**
0	D:D	6.714
0	H:D	5.167
0	D:H	3.061
1	D:D:D	6.634
1	H:D:D	5.474
1	D:H:D	3.894
2	D:D:D	6.585
2	H:D:D	5.658
2	D:H:D	4.394
5	D:D:D	6.513
5	H:D:D	5.933
5	D:H:D	5.144
10	D:D:D	6.467
10	H:D:D	6.110
10	D:H:D	5.624

SasView was generally used for fitting,[4] while the Teubner-Strey model was implemented in Python using SciPy.[5] Several different models were first trialled in fitting to establish the most appropriate structural representation (Figure S1). The Guinier approximation gave a decent fit to the radius for low-water systems (signifying more globular aggregates), but was clearly missing a term to represent intermicellar interactions, such as a structure factor, S(Q). We also considered the propensity of

AOT for forming reverse micelles;[6] this gave a reasonable solution for the low-water data, but did not match perfectly at high-Q or low-Q, and did not propagate across all datasets. A short cylinder, or oblate ellipsoid, gave the best fit to most datasets, except those at high water contents and low AOT concentrations, which fitted best to an infinite lamellar sheet, where the radius of the disc exceeded the available instrumental Q-range. Any low-Q mismatch is assigned to multiple aggregates which were not modelled, worse signal:noise at the low-Q limit, and difficulties in background corrections. In terms of fitted parameters, the core and solvent SLDs were always fixed, leaving 5 free parameters for the simple oblate ellipsoid, 3 free parameters for the lamellar model, 8 free parameters for the core-shell ellipsoid (*i.e.* reverse micelle), and 7 free parameters for the core-shell cylinder. Where it was not possible to fit systems adequately using the full gamut of completely free-floating parameters, such as those with a Δ_{SLD} term (describing scattering contrast between the solvent bulk and micelle core) of $<1\times10^{-6}$ Å^{-2}, a local fitting minimum was first found by applying the mean micellar polar radii (R_{po}) calculated from fits of other samples with $\Delta_{SLD} >1\times10^{-6}$ Å^{-2}, with the standard deviation of this population then used as a constraint for a subsequent fit, allowing R_{po} to vary between 7.864 Å $\leq R_{po} \leq$ 10.506 Å. All models are freely available from the SasView documentation.[4]

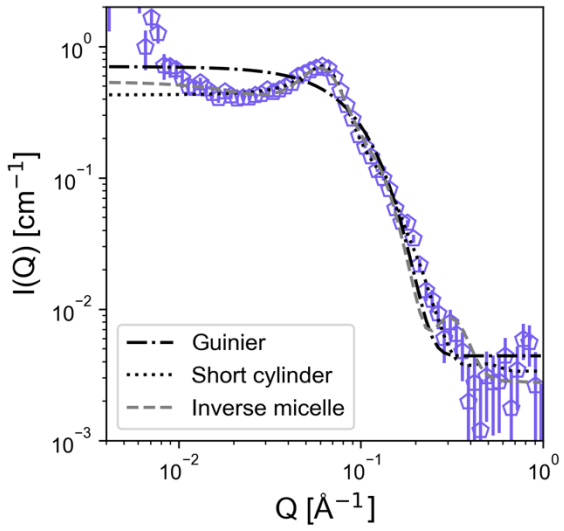

Figure S1. Best fits obtained during a comparison of different models trialled for fitting, upon the D:D:H 0*w* 1 wt.% AOT data (light grey pentagons), prior to settling on an oblate ellipsoid with Percus-Yevick S(Q) for mass data fitting, and short core-shell cylinder with Percus-Yevick S(Q) for constrained simultaneous fits to obtain micelle fine structure. Examples include a Guinier fit with R_g = 17.79 Å; a core-shell ellipsoid fit with hard sphere S(Q), core SLD of the solvent, and shell SLD of the surfactant tails (*i.e.* an inverse micelle, which AOT often forms), which gave a core radius of 5.22 Å and shell thickness of 11.5 Å; a short simple cylinder with hard sphere S(Q), of R_{eq} = 57.92 Å, length = 17.77 Å.

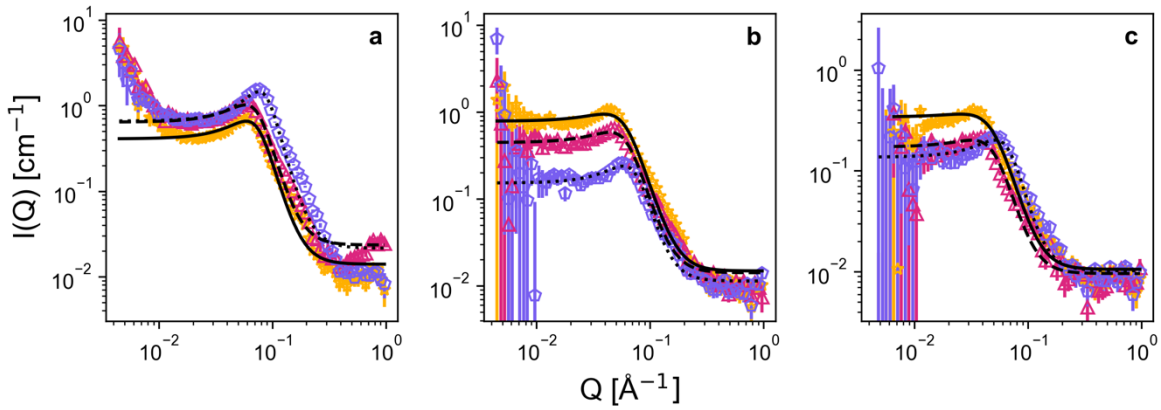

Figure S2. Small-angle neutron scattering (SANS) data from samples containing H-AOT and perdeuterated DES, showing best fits of the Teubner-Strey microemulsion model at compositions of *w*=0 (a), *w*=1 (b) and *w*=2 (c). Data are shown as purple pentagons (1 wt.% AOT), magenta upwards triangles (2 wt.% AOT) and gold stars (5 wt.% AOT), with corresponding fits shown as black dotted, dashed, and solid lines, respectively.

Fitting parameters

Table S2. Fitted parameters for the samples containing D-choline chloride, D-urea, and D_2O (except for 0*w*, which is dry), and H-AOT. All samples were fit with a simple oblate ellipsoid model and a Percus-Yevick hard sphere structure factor, except samples shown as $R_{eq} = \infty$, which were fitted to a uniform lamellar model with no intermicellar potential.

[AOT] [wt.%]	[*w*] [mol. eqv.]	Contrast [ChCl:urea :(water):AOT-tail]	ϕ	R_{po} [Å]	R_{eq} [Å]	ϕ_{HS}
1	0	D:D:H	0.017±0.000	9.443±0.219	62.834±0.311	0.281±0.002
2	0	D:D:H	0.024±0.000	10.321±0.155	63.092±0.237	0.279±0.001
5	0	D:D:H	0.051±0.000	9.305±0.087	52.808±0.111	0.317±0.001
1	1	D:D:D:H	0.017±0.000	9.111±0.225	83.258±0.384	0.263±0.002
2	1	D:D:D:H	0.011±0.000	9.191±0.334	78.512±0.520	0.264±0.002
5	1	D:D:D:H	0.007±0.000	8.599±0.607	63.439±0.783	0.275±0.004
1	2	D:D:D:H	0.004±0.000	8.871±0.819	104.510±1.375	0.248±0.005
2	2	D:D:D:H	0.003±0.000	8.451±1.370	99.540±1.989	0.258±0.008
5	2	D:D:D:H	0.005±0.000	9.122±0.804	71.018±1.072	0.273±0.005
1	5	D:D:D:H	0.005±0.001	9.620±0.842	156.920±4.316	0.145±0.010
2	5	D:D:D:H	1.769±NaN	9.298±1.613	124.040±12.470	0.000±0.033
5	5	D:D:D:H	0.010±0.000	9.322±0.348	108.650±0.775	0.232±0.003
1	10	D:D:D:H	0.007±0.000	9.118±0.068	∞	-
2	10	D:D:D:H	0.012±0.000	8.739±0.044	∞	-
5	10	D:D:D:H	0.194±0.001	9.619±0.030	234.670±0.423	0.193±0.001

Table S3. Fitted parameters for the samples containing H-choline chloride, D-urea, and D_2O (except for 0*w*, which is dry), and D-AOT. All samples were fit with a simple oblate ellipsoid model and a Percus-Yevick hard sphere structure factor, except samples shown as $R_{eq} = \infty$, which were fitted to a uniform lamellar model with no intermicellar potential.

[AOT] [wt.%]	**[*w*] [mol. eqv.]**	**Contrast [ChCl:urea :(water):AOT-tail]**	**ϕ**	**R_{po} [Å]**	**R_{eq} [Å]**	**ϕ_{HS}**
1	0	H:D:D	0.137±0.014	11.218±1.411	64.903±1.818	0.286±0.009
2	0	H:D:D	0.253±0.037	7.650±1.229	64.644±1.479	0.272±0.007
5	0	H:D:D	0.530±0.037	7.425±0.578	55.281±0.577	0.313±0.004
1	1	H:D:D:D	0.242±0.040	9.193±1.649	87.328±2.321	0.260±0.009
2	1	H:D:D:D	0.624±0.058	7.864±0.796	79.047±1.012	0.271±0.005
5	1	H:D:D:D	0.818±0.055	8.030±0.610	59.199±0.655	0.304±0.004
1	2	H:D:D:D	0.244±0.093	7.864±3.129	136.820±5.129	0.233±0.014
2	2	H:D:D:D	0.158±0.115	7.864±6.235	90.435±11.412	0.202±0.038
5	2	H:D:D:D	0.406±0.085	8.114±1.887	66.191±2.046	0.296±0.011
1	5	H:D:D:D	0.443±0.855	7.864±10.803	164.070±77.719	0.092±0.150
2	5	H:D:D:D	0.430±0.455	7.864±8.204	164.520±36.275	0.127±0.071
5	5	H:D:D:D	0.667±0.308	7.864±3.834	127.590±8.289	0.191±0.022
1	10	H:D:D:D	0.325±0.088	7.864±2.172	∞	-
2	10	H:D:D:D	0.648±0.089	7.864±1.101	∞	-
5	10	H:D:D:D	16.328±1.108	7.864±0.471	265.170±2.507	0.189±0.004

Table S4. Fitted parameters for the samples containing D-choline chloride, H-urea, and D_2O (except for 0*w*, which is dry), and D-AOT. All samples were fit with a simple oblate ellipsoid model and a Percus-Yevick hard sphere structure factor, except samples shown as $R_{eq} = \infty$, which were fitted to a uniform lamellar model with no intermicellar potential.

[AOT] [wt.%]	[*w*] [mol. eqv.]	Contrast [ChCl:urea :(water):AOT-tail]	ϕ	R_{po} [Å]	R_{eq} [Å]	ϕ_{HS}
1	0	D:H:D	0.007±0.001	10.880±2.532	66.064±2.537	0.339±0.015
2	0	D:H:D	0.020±0.002	10.513±1.247	59.162±1.521	0.292±0.008
5	0	D:H:D	0.002±0.001	10.770±0.451	51.624±0.506	0.317±0.003
1	1	D:H:D:D	0.032±0.004	10.388±1.314	75.007±2.100	0.244±0.009
2	1	D:H:D:D	0.049±0.004	9.477±0.932	65.888±1.227	0.272±0.006
5	1	D:H:D:D	0.070±0.003	10.096±0.618	54.622±0.711	0.305±0.004
1	2	D:H:D:D	0.050±0.026	5.782±3.104	103.450±4.545	0.212±0.014
2	2	D:H:D:D	0.046±0.031	5.140±3.549	98.596±3.479	0.262±0.012
5	2	D:H:D:D	0.108±0.006	9.309±0.627	68.377±0.818	0.278±0.004
1	5	D:H:D:D	0.289±0.366	7.864±2.586	178.280±37.260	0.057±0.068
2	5	D:H:D:D	0.023±0.028	7.864±9.653	161.900±21.673	0.191±0.048
5	5	D:H:D:D	0.026±0.004	10.505±0.000	127.990±10.769	0.206±0.032
1	10	D:H:D:D	0.019±0.004	9.469±2.190	∞	-
2	10	D:H:D:D	0.041±0.004	9.500±1.039	∞	-
5	10	D:H:D:D	1.202±0.057	9.815±0.409	198.470±2.400	0.165±0.005

Table S5. Estimation of the micelle shell composition from the simultaneous constrained fits of the three 1wt.% AOT, 0*w* DES contrasts, to the core-shell cylinder model. The mole fractions X_{ChCl} and X_{urea} were optimised by least-squares fitting to obtain the listed shell profiles.

[AOT] [wt.%]	[*w*] [mol. eqv.]	Contrast [ChCl:urea :AOT-tail]	$SLD_{shell,model}$ [x10^{-6} Å^{-2}]	$X_{AOT,shell}$	$X_{ChCl,shell}$	$X_{Urea,shell}$
1	0	D:D:H	3.889±1.621	0.859	0.042	0.099
1	0	H:D:D	3.345±1.403	0.859	0.042	0.099
1	0	D:H:D	5.167±0.575	0.582	0.000	0.418

References

(1) Hammond, O. S.; Bowron, D. T.; Edler, K. J. The Effect of Water upon Deep Eutectic Solvent Nanostructure: An Unusual Transition from Ionic Mixture to Aqueous Solution. *Angew. Chem. - Int. Ed.* **2017**, No. 56, 9782–9785. https://doi.org/10.1002/anie.201702486.

(2) Atri, R.; Sanchez-Fernandez, A.; Hammond, O. S.; Manasi, I.; Doutch, J.; Tellam, J. P.; Edler, K. J. Morphology Modulation of Ionic Surfactant Micelles in Ternary Deep Eutectic Solvents. *J. Phys. Chem. B* **2020**, *124*, 6004–6014. https://doi.org/10.1021/acs.jpcb.0c03876.

(3) Caponetti, E.; Chillura-Martino, D.; Ferrante, F.; Pedone, L.; Ruggirello, A.; Turco Liveri, V. Structure of Urea Clusters Confined in AOT Reversed Micelles. *Langmuir* **2003**, *19* (12), 4913–4922. https://doi.org/10.1021/la027066n.

(4) SasView. http://www.sasview.org/.

(5) Virtanen, P.; Gommers, R.; Oliphant, T. E.; Haberland, M.; Reddy, T.; Cournapeau, D.; Burovski, E.; Peterson, P.; Weckesser, W.; Bright, J.; van der Walt, S. J.; Brett, M.; Wilson, J.; Millman, K. J.; Mayorov, N.; Nelson, A. R. J.; Jones, E.; Kern, R.; Larson, E.; Carey, C. J.; Polat, İ.; Feng, Y.; Moore, E. W.; VanderPlas, J.; Laxalde, D.; Perktold, J.; Cimrman, R.; Henriksen, I.; Quintero, E. A.; Harris, C. R.; Archibald, A. M.; Ribeiro, A. H.; Pedregosa, F.; van Mulbregt, P.; SciPy 1.0 Contributors; Vijaykumar, A.; Bardelli, A. P.; Rothberg, A.; Hilboll, A.; Kloeckner, A.; Scopatz, A.; Lee, A.; Rokem, A.; Woods, C. N.; Fulton, C.; Masson, C.; Häggström, C.; Fitzgerald, C.; Nicholson, D. A.; Hagen, D. R.; Pasechnik, D. V.; Olivetti, E.; Martin, E.; Wieser, E.; Silva, F.; Lenders, F.; Wilhelm, F.; Young, G.; Price, G. A.; Ingold, G.-L.; Allen, G. E.; Lee, G. R.; Audren, H.; Probst, I.; Dietrich, J. P.; Silterra, J.; Webber, J. T.; Slavič, J.; Nothman, J.; Buchner, J.; Kulick, J.; Schönberger, J. L.; de Miranda Cardoso, J. V.; Reimer, J.; Harrington, J.; Rodríguez, J. L. C.; Nunez-Iglesias, J.; Kuczynski, J.; Tritz, K.; Thoma, M.; Newville, M.; Kümmerer, M.; Bolingbroke, M.; Tartre, M.; Pak, M.; Smith, N. J.; Nowaczyk, N.; Shebanov, N.; Pavlyk, O.; Brodtkorb, P. A.; Lee, P.; McGibbon, R. T.; Feldbauer, R.; Lewis, S.; Tygier, S.; Sievert, S.; Vigna, S.; Peterson, S.; More, S.; Pudlik, T.; Oshima, T.; Pingel, T. J.; Robitaille, T. P.; Spura, T.; Jones, T. R.; Cera, T.; Leslie, T.; Zito, T.; Krauss, T.; Upadhyay, U.; Halchenko, Y. O.; Vázquez-Baeza, Y. SciPy 1.0: Fundamental Algorithms for Scientific Computing in Python. *Nat. Methods* **2020**, *17* (3), 261–272. https://doi.org/10.1038/s41592-019-0686-2.

(6) Kotlarchyk, M.; Huang, J. S.; Chen, S. H. Structure of AOT Reversed Micelles Determined by Small-Angle Neutron Scattering. *J. Phys. Chem.* **1985**, *89* (20), 4382–4386. https://doi.org/10.1021/j100266a046.